coatings

MDPI

Article

Mechanical Grinding of Hydroxyapatite and Its Interaction with Titanium

Axaule Mamaeva, Aidar Kenzhegulov *, Aleksander Panichkin, Rinat Abdulvaliyev, Balzhan Kshibekova and Talgat Arynbayev

The Institute of Metallurgy and Ore Beneficiation, JSC, Satbayev University, NJSC, Almaty 050013, Kazakhstan; ak78@mail.ru (A.M.); a.panichkin@satbayev.university (A.P.); rin-abd@mail.ru (R.A.); b.kshibekova@satbayev.university (B.K.); kazak.t91@mail.ru (T.A.)

* Correspondence: a.kenzhegulov@satbayev.university; Tel.: +7-707-200-00-62

Abstract: The development of promising biocompatible composites based on hydroxyapatite with a metallic component is of great interest to researchers. This article describes the synthesis of hydroxyapatite powder by the hydrolytic method and presents the results of mechanical grinding of hydroxyapatite powder. Additionally, in order to study the interaction between titanium and hydroxyapatite powders, the results of their thermal treatment in the temperature range of 600–900 °C are presented. As a result of the hydrolytic method, a powder consisting of $Ca_5(PO_4)_3(OH)$ and CaO phases with a fraction of 400–600 μm was obtained. According to the results of mechanical grinding, it was determined that with an increase in grinding time from 30 to 120 min, the intensive main diffraction lines corresponding to hydroxyapatite decrease. During the thermal treatment of titanium and hydroxyapatite powders, titanium oxidizes forming suboxides and titanium dioxide (TiO_2). At higher temperatures, the hydroxyapatite phase disappears from the mixture, and titanium oxide, calcium phosphate compound, and small amounts of calcium titanate and titanium hydrophosphate are present.

Keywords: mechanical grinding; hydroxyapaptite; titanium; structure; heat treatment

check for updates

Citation: Mamaeva, A.; Kenzhegulov, A.; Panichkin, A.; Abdulvaliyev, R.; Kshibekova, B.; Arynbayev, T. Mechanical Grinding of Hydroxyapatite and Its Interaction with Titanium. *Coatings* **2024**, *14*, 333. https://doi.org/10.3390/coatings14030333

Academic Editor: Simona Iconaru

Received: 6 February 2024
Revised: 5 March 2024
Accepted: 10 March 2024
Published: 12 March 2024

Copyright: © 2024 by the authors. Licensee MDPI, Basel, Switzerland. This article is an open access article distributed under the terms and conditions of the Creative Commons Attribution (CC BY) license (https://creativecommons.org/licenses/by/4.0/).

1. Introduction

In medical practice, implants are used to correct bone defects or replace damaged tissue. However, selecting the optimal balance of implant strength characteristics, with maximum biological compatibility, remains one of the most important unresolved issues [1,2]. To mitigate the negative impact of these factors, it is necessary to create a transitional zone between the bone and the implant, which, alongside a strong bond with the implant material, should possess an organism-acceptable macro- and microstructure. Coatings on metals, characterized by specific porosity and developed morphology, required for effective implant integration, can serve this purpose [3–5].

For this task, composite materials based on hydroxyapatite (HA) and titanium [6,7] are considered the most promising, as they are bioactive and possess high mechanical characteristics [8–11]. Hydroxyapatite is the most suitable bone substitute material, characterized by excellent biocompatibility with bone tissue. Consequently, it serves as a fundamental component in orthopedics and dentistry [12,13]. Hydroxyapatite resembles the biological mineral providing skeletal strength and serving as a reservoir for calcium, phosphorus, sodium, and magnesium. It is known that there exists an inverse relationship between the biological and mechanical properties of biomaterials: the better the tissue accepts the implanted material, the worse its mechanical properties [14,15].

The interaction of HA with living tissue depends on its chemical composition, size, and morphology [16]. Therefore, synthesizing a synthetic analog of the bone's mineral component is a relevant and demanded task. Developing methods for the synthesis and

processing of biocompatible materials of specified composition and morphology poses a significant challenge.

Commonly used methods for obtaining HA mainly include hydrothermal, precipitation, solvothermal, self-combustion, microemulsion, ultrasound synthesis, electrochemical synthesis, biomimetic, and solid-state reaction methods, namely wet and dry methods. Among them, the most widely used methods for obtaining HA powders in recent years are hydrothermal, thermal solvent, and precipitation methods [17]. However, researchers have been constantly modifying the corresponding methods and subsequent processing of nanoscale hydroxyapatite and its composite materials to achieve the desired biological and mechanical properties.

The crystallinity of HA for hard tissue regeneration has been controlled by mechanical grinding (MG) methods and subsequent heat treatment. For instance, in [18], crystallinity, based on crystallite size and elastic deformation of crystals, decreased over time of grinding, and the rate of decrease depended on the type of calcium phosphate. Researchers in [19] found that after 72 h of grinding, the main peak of HA became completely invisible on the diffractogram. Dinda S. and colleagues [20] reported on the progress of the mechanochemical synthesis of nanocrystalline HA from six different powder mixtures containing $Ca(H_2PO_4)_2 \cdot H_2O$, CaO, $Ca(OH)_2$, and P_2O_5. The rate of mechanochemical reaction of the powder mixture $Ca(H_2PO_4)_2 \cdot H_2O$–$Ca(OH)_2$ was very high, as the HA phase began to form approximately after 2 min and was completed after 30 min of grinding in a ball mill. All six powder mixtures were completely transformed into HA with crystallite sizes ranging from 18.5 to 20.2 nm after 1 h and from 22.5 to 23.9 nm after 2 h of grinding. In [21], hydroxyapatite coatings on titanium were obtained after mechanochemical interaction by the gas-dynamic spraying method. The results of cross-sections of coatings showed that the formation of HA particles predominantly occurred in the depressions of the titanium substrate. After spraying, the composition of the HA layer did not undergo significant changes.

In the scientific literature, there is a limited amount of research discussing the interaction of titanium with hydroxyapatite. For instance, in studies [22–24], it has been noted that the dehydroxylation process of hydroxyapatite becomes more intensive in the presence of titanium atoms, facilitating the diffusion of oxygen into metallic titanium and the formation of titanium oxides. Additionally, calcium and phosphorus ions migrate into the substrate from titanium, affecting the Ca/P ratio in the apatite. Phosphorus ions exhibit a higher migration rate due to their smaller radius and lower activation energy. Other researchers report the presence of calcium, phosphorus, and titanium atoms in certain areas, but no other phases resulting from the reaction between hydroxyapatite and TiO_2 have been detected. The presence of calcium, phosphorus, and titanium atoms indicates mutual diffusion in the HA/Ti composite [22,25].

Despite the available research, the interaction of components at the interface of metal (alloy)–hydroxyapatite is hardly studied, although it determines the subsequent physicomechanical properties and biocompatibility of the implant with the body tissues. Therefore, it is necessary to conduct studies of physicochemical processes occurring in relevant systems, which is highly relevant. Since coatings of metal implants with hydroxyapatite often delaminate due to the low surface energy of the interface between the ceramic and the metal, which can lead to surgical failure, this problem can be addressed by manufacturing a metal/HA composite. Our goal was to obtain a metal/HA composite at the interface. The aim of the research was to study the processes of interaction between HA and titanium during heat treatment. Evaluating the influence of these processing methods on the structure and phase composition of the Ti + HA mixture will contribute to the development of new surface treatment methods for endoprostheses.

2. Materials and Methods

2.1. Synthesis of Hydroxyapatite

The hydrolytic synthesis method was employed in the present study to obtain HA powder. For this purpose, a mixture of dicalcium phosphate dihydrate $CaHPO_4 \cdot 2H_2O$, DHHCP (Sigma-Aldrich, St. Louis, MA, USA), and calcium carbonate ($CaCO_3$ (Sigma-Aldrich)) was added to a 500 mL aqueous 10% NaOH solution and vigorously stirred at 75 °C for 1 h. The solution stirring was performed using a DLS overhead stirrer (Velp scientifica, Monza, Italy) operating at a speed of 1000 revolutions per minute. The reaction was quenched by cooling in an ice bath. Subsequently, the solution was filtered, washed, and dried at 60 °C. Since DCPD and $CaCO_3$ are poorly soluble in water, the hydrolysis process serves as a rapid means of dissolving the solid phase at elevated pH = 8–9 and temperatures above 60 °C. The obtained precipitate of powder was collected, washed, and subjected to drying. Fractionation through a sieve set yielded a fraction of 400–600 μm, which was utilized in subsequent experiments.

2.2. Mechanical Grinding of Hydroxyapatite

The dried powders intended for treatment via MG were placed into the container of a ball mill along with several balls. The mixture of HA powders of the specified chemical composition inside a chamber with a volume of 20 cm^3, together with steel balls, was subjected to vibrational motion within a defined frequency range of 60 Hz for the processed material. The grinding process was conducted for durations ranging from 30 to 120 min. Following the MG process, the preferred powder of HA was selected for further investigation of its interaction with titanium.

2.3. Sintering of Titanium and Hydroxyapatite Powders

To investigate the interaction between HA and titanium, the mixture of these powders underwent a process of pressing and sintering. The mixture of HA and titanium powders was subjected to uniaxial pressing at pressures ranging from 120 to 150 MPa at room temperature in a metallic die to obtain raw specimens with a diameter of 15 mm and a height of 4 mm. These specimens were then air-dried for 24 h. A water-based starch solution was used as a binder, as its addition to the powder mixture in a mass ratio of 5% practically did not alter the phase composition of the original powder.

Subsequently, the HA-Ti mixture was sintered at temperatures ranging from 600 to 1100 °C with an isothermal hold for 1 h at each temperature. To prevent titanium oxidation, the sintering process was conducted in a protective argon atmosphere.

2.4. Research Methods

The morphology and microstructure of the obtained specimens were analyzed in transmitted light in an immersion medium under an OLYMPUS microscope BX51 (Olympus Corporation, Tokyo, Japan) on a scanning electron microscope equipped with an energy-dispersive X-ray spectroscopy (EDS) attachment (Jeol–JXA8230, Tokyo, Japan), and on an atomic force microscope (AFM PSIA XE-100, Sungnam, Republic of Korea). Particle sizes of the powders were determined using ImageJ software (1.53q). X-ray diffraction patterns were obtained using a D8 Advance diffractometer (Bruker, Ettlingen, Germany) with α–Cu radiation, with scans performed in the angular range from 4° to 90°. Radiography was performed with focusing according to the Bragg–Brentano method. The PDF 2 database was used for phase analysis.

3. Results and Discussion

3.1. Synthesis and Mechanical Grinding of Hydroxyapatite

Figure 1 shows the X-ray diffraction pattern of the HA powder obtained by the hydrolytic synthesis method prior to mechanical grinding. The results indicate the presence of the phases $Ca_5(PO_4)_3(OH)$ and CaO in the HA powder. The main phase of the initial HA is characterized by dominant crystallographic orientations (002), (211), and (300).

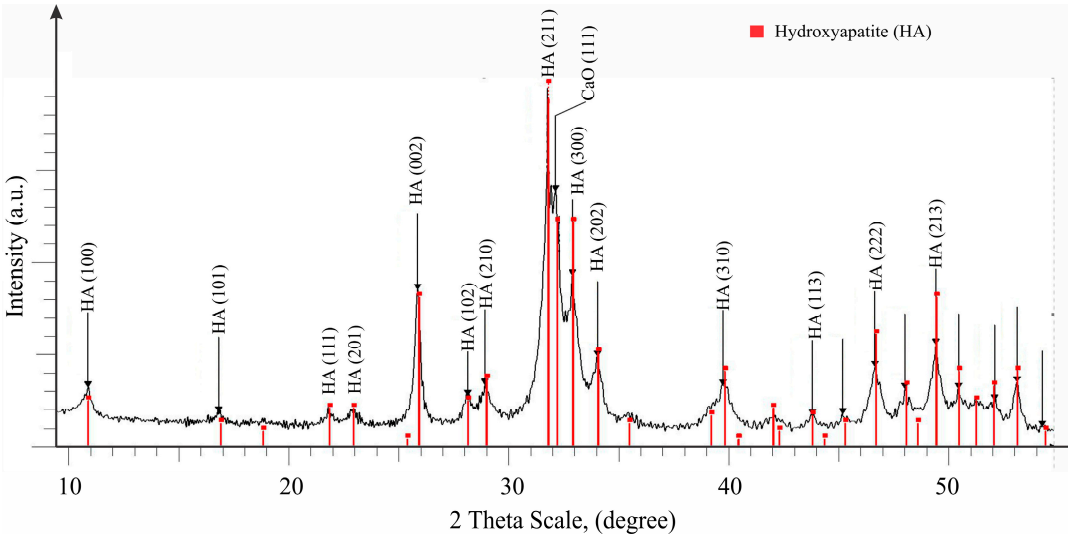
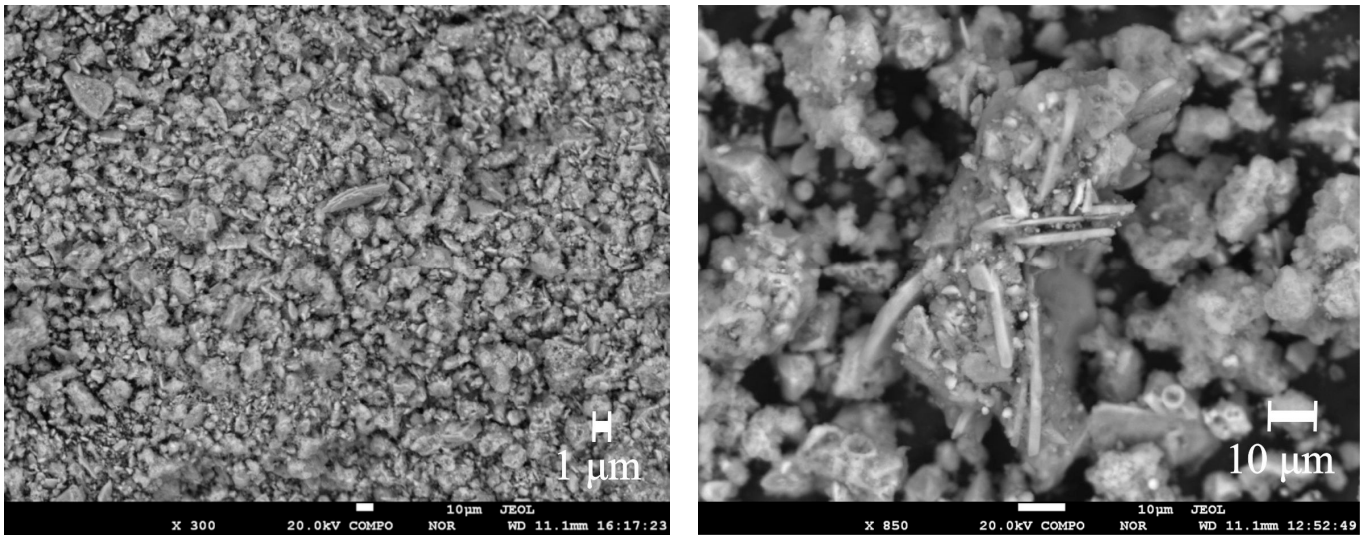


Figure 1. X-ray pattern of hydroxyapatite powder before grinding.

For obtaining high-quality powders, an important factor influencing mechanical comminution is the grinding time. SEM images of HA powder obtained after 30 and 50 min are presented in Figure 2. The morphological image in backscattered electrons of HA powder particles after 30 min of grinding (Figure 2a) demonstrates a uniform distribution of particles ranging in size from 520 nm to 10 μm. With further increasing grinding time, the number of particles with small sizes up to 2 ± 1.4 μm increases, and larger particles up to 35 ± 5 μm become noticeable. However, prolonging the grinding time leads to contamination of the material with steel elements from the grinding container. This was determined by EDS analysis. This is due to the fact that during grinding, the container is also subjected to mechanical stress, which can result in wear and corrosion of its surface. As a result, steel elements may be released from the container surface and contaminate the material being ground [26]. Morphologically, in the HA ground for 50 min (Figure 2b), small agglomerate clusters and, in some areas, individual needle-like structures can be observed. The morphology of deposited HA can vary from needle-like to granular depending on the grinding time. Thus, particles acquire smaller sizes due to fragmentation and agglomerate through mechanical grinding.



(**a**) (**b**)

Figure 2. Morphology and particle size of HA powder particles ground for: (**a**) 30; (**b**) 50 min.

When the phase composition of the powder was studied depending on the grinding time, it was found that the main phase was HA in all samples (Figure 3). The peaks corresponding to HA from the crystallographic orientations (002), (211), and (112) were prominently displayed. The main diffraction lines corresponding to HA shift towards larger angles with the increase in grinding time, and the interplanar distances decrease, which apparently indicates the process of dehydration and disorder of the HA structure. With increasing grinding time, the X-ray diffraction patterns also showed a broadening and decreasing intensity of the peaks attributed to HA reflection. This indicates a decrease in the size of the crystallites of the phase under study, and this can be caused by dislocation-type lattice defects [27]. Additionally, it was observed from the X-ray diffractograms that the powders remained crystalline. After grinding for a period ranging from 50 to 120 min, no broadening of peaks or reduction in intensity were observed in the diffractograms.

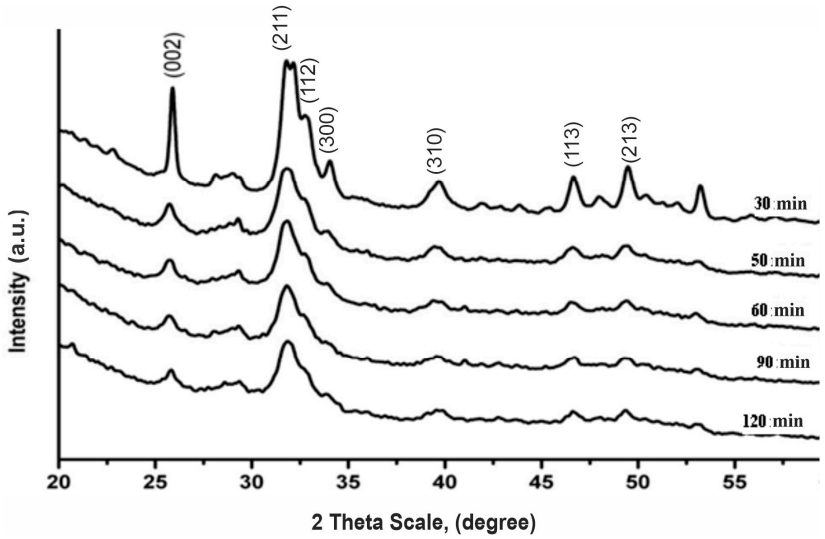
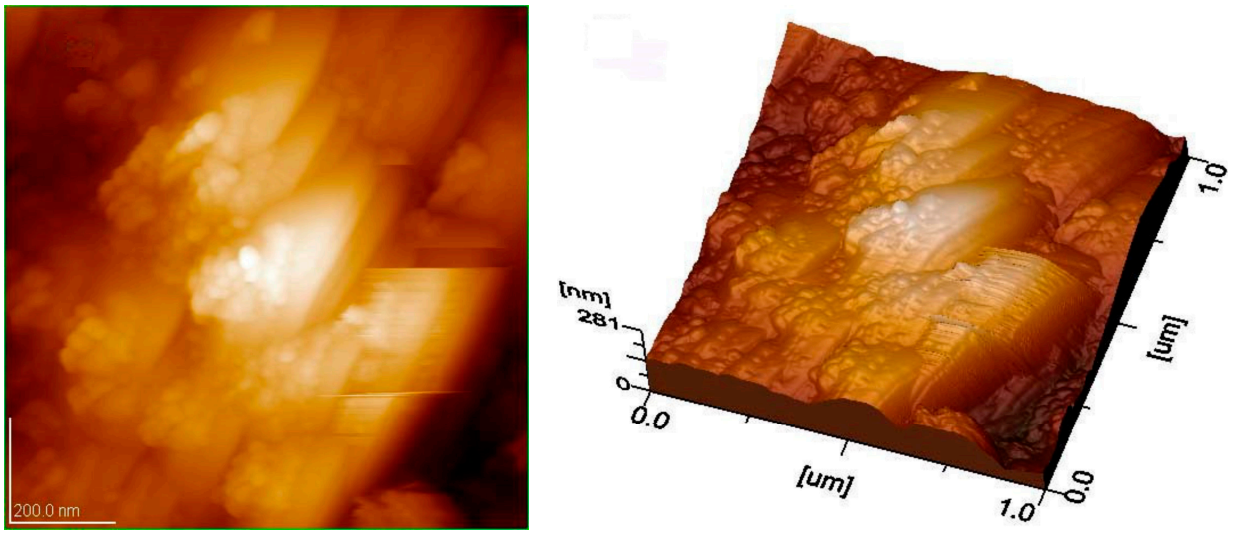


Figure 3. X-ray patterns of HA powder ground for different times.

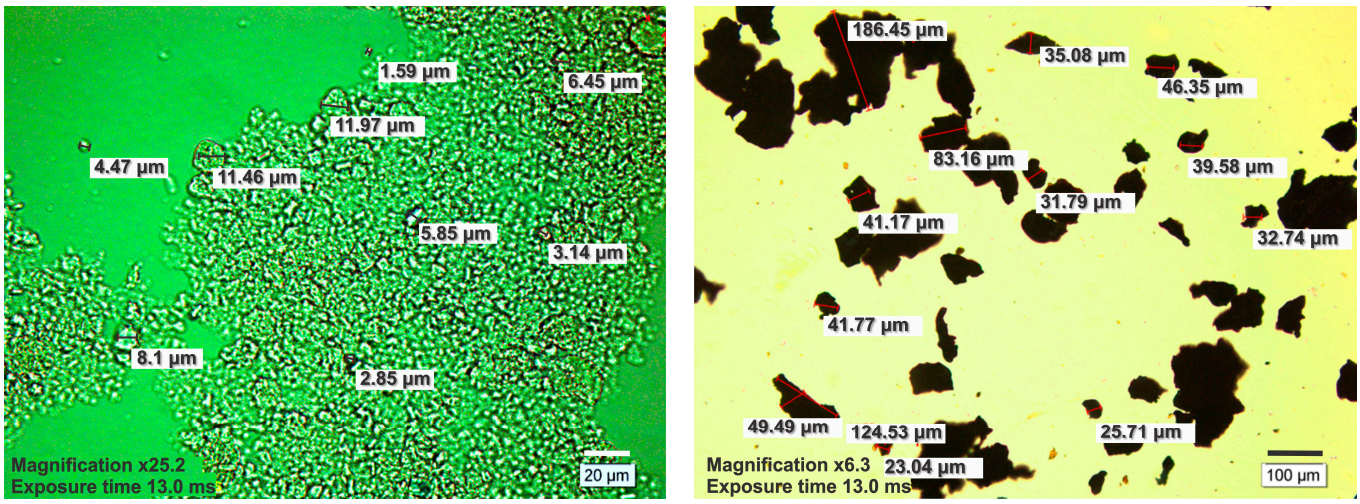
An AFM image of the HA powder after grinding for 120 min shows (Figure 4) that the material consists of numerous spherical aggregates of various sizes, ranging from 10 μm to 200 nanometers, with some being significantly smaller. Each spherical aggregate, in turn, consists of numerous grains. Surface scanning of the HA indicated that the height of its particles reached up to 281 nm (Figure 4b).



(**a**) (**b**)

Figure 4. AFM images of HA powder after grinding for 120 min: (**a**) 2D; (**b**) 3D.

In light of the contamination of the HA powder with an increase in the processing time of MG and the results of the X-ray diffraction patterns, it was proposed to select HA powder subjected to 30 min of grinding for the subsequent stage—investigating its interaction with titanium. The optical micrographs in Figure 5 depict the powders in their original state, showing agglomerated HA particles ranging in size from 2 to 12 µm (Figure 5a), and titanium particles with irregular shapes, varying in size from 20 to 186 µm (Figure 5b).



(**a**) (**b**)

Figure 5. Powder structures in the initial state: (**a**) HA; (**b**) Ti.

3.2. Sintering of Titanium and Hydroxyapatite Powders

The interaction between titanium and hydroxyapatite has been studied in the following works [28,29]. According to the results of these studies, titanium oxidizes due to its interaction with oxygen in HA. At the interface between HA and Ti, titanium atoms undergo oxidation to form TiO_2, typically on the upper part of the titanium surface, at elevated temperatures. However, changes in processing parameters can alter the passivation of TiO_2 formation. In such cases, titanium atoms from the metallic bulk migrate and interact with HA, while oxygen atoms penetrate into titanium. As a result of this process, TiO_2 is formed in either an amorphous or crystalline form. The kinetics of titanium oxidation depend on the rate of oxygen adsorption, which diffuses into the titanium lattice until saturation is reached, after which oxidation begins. The rate of oxygen diffusion slows down upon the formation of TiO_2 [22,30].

As a result of pressing and sintering at various temperatures, different crystalline phases are formed in the titanium and HA powder mixtures. As shown in Figure 6a, after sintering at 600 °C, localized large titanium particles and a large number of small HA particles can be observed. At higher temperatures of 900–1100 °C (Figure 6d–f), the quantity of small HA particles decreases. From around 700 °C (Figure 6b), finely pronounced small cracks begin to appear. The appearance of cracks during the sintering of hydroxyapatite and titanium powders is attributed to several factors. One of these factors is the decomposition of HA at high temperatures within the composite material [31]. Pure HA remains stable up to 1200 °C in an argon atmosphere, but when considering sintered HA/Ti, titanium ions react with hydroxyl groups in HA, forming titanium oxide, thereby accelerating dehydroxylation and decomposition of HA at approximately 800 °C [22].

As shown in the diffraction patterns in Figure 7, the initial HA-Ti mixture exhibits peaks characteristic of titanium and broad peaks in the range of 31–34° corresponding to HA. After thermal treatment of the HA-Ti system at 700 °C, the main peak of Ti shifts towards smaller angles, which may be attributed to the formation of a solid solution of oxygen in titanium and titanium suboxide $TiO_{0.325}$ (characteristic peak at 39.98°). Additionally, a weak intensity peak of TiO_2 appears around 27°. At 800 °C, there is an increase in the

intensity of TiO_2 diffraction peaks. For the HA-Ti system at temperatures above 800 °C, simultaneous decomposition of HA and oxidation of titanium occur, which completes at 900 °C. As a result of the interaction between titanium oxide and decomposition products of HA, titanium oxide, calcium phosphate compound, and small amounts of calcium titanate and titanium hydrophosphate are formed.

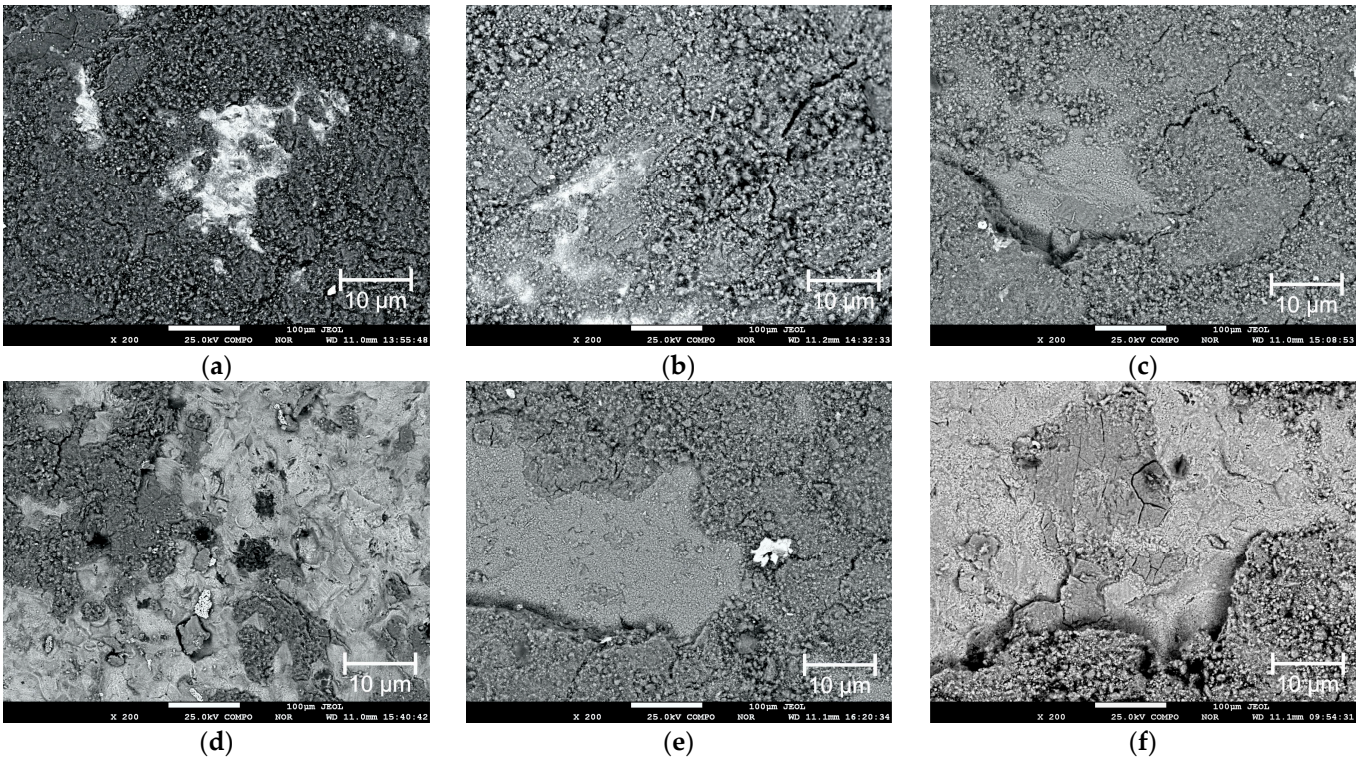


Figure 6. Structure of sintered powders of hydroxyapatite and titanium at different temperatures: 600 °C (**a**); 700 °C (**b**); 800 °C (**c**); 900 °C (**d**); 1000 °C (**e**); 1100 °C (**f**).

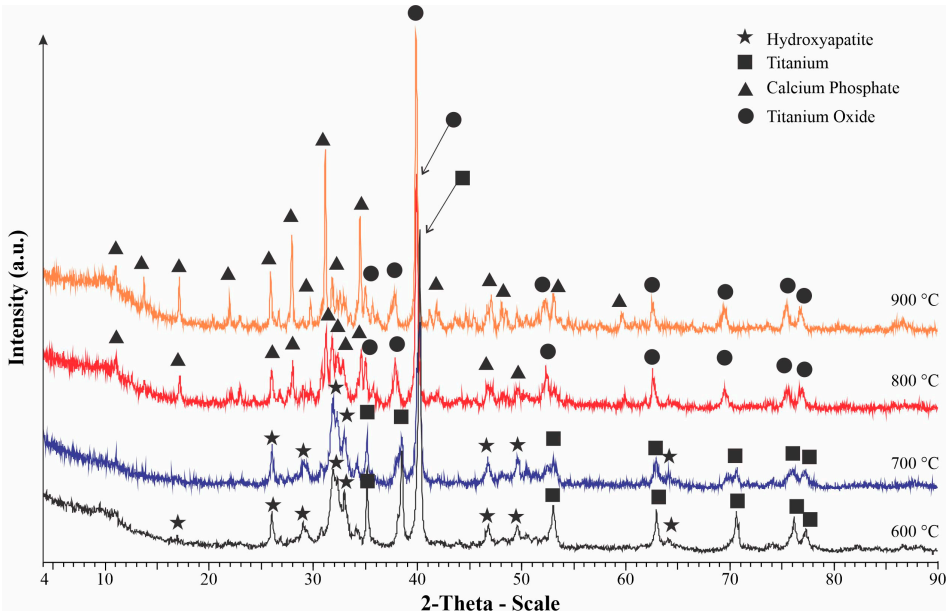


Figure 7. X-ray diffraction analysis of sintered hydroxyapatite and titanium powder at various temperatures.

4. Conclusions

It was established as a result of this work that the hydrolytic synthesis of hydroxyapatite produces a powder consisting of $Ca_5(PO_4)(OH)$ and CaO phases with a fraction of 400–600 μm. After mechanical grinding, the main phase of the powder consists of $Ca_{10}(PO_4)_3(OH)$. Depending on the grinding time, the fractional composition is in the range from 35 μm to 520 nm. Therefore, an important factor affecting particle size and composition is the duration of mechanical grinding. The main final product of the interaction between HA and Ti mainly consists of two phases—titanium oxide and calcium phosphate compound. The oxidation of titanium to suboxide at 700 °C and its complete oxidation to TiO_2 after 800 °C is common to the two composite systems under consideration. As a result, it is not possible to retain titanium metal as a dispersed reinforcing component of the composite material during the sintering of the HA–Ti composite mixture.

The presented results in the study on the interaction between hydroxyapatite and titanium powders could serve as a stimulus for seeking improved materials for implants. Discussing these results may draw researchers' attention to the necessity of enhancing biocomposites based on hydroxyapatite and titanium to improve the efficiency and effectiveness of implant utilization.

Author Contributions: Conceptualization, A.M. and A.P.; methodology, A.K. and B.K.; software, A.K.; validation, A.M., A.P. and A.K.; formal analysis, B.K.; investigation, A.M.; resources, T.A.; data curation, A.K.; writing—original draft preparation, A.M.; writing—review and editing, A.K. and T.A.; visualization, R.A. and A.P.; supervision, R.A.; project administration, A.M.; funding acquisition, R.A. All authors have read and agreed to the published version of the manuscript.

Funding: This research was funded by the Committee of Science of the Ministry of Education and Science of the Republic of Kazakhstan within Program-Targeted Funding, grant number BR18574018.

Institutional Review Board Statement: Not applicable.

Informed Consent Statement: Not applicable.

Data Availability Statement: The data and results presented in this study are available in the article.

Acknowledgments: The authors are grateful to the National Laboratory for Collective Use of Institute of Metallurgy and Ore Beneficiation JSC for the analysis of the samples with the use of electron microscopy, X-ray phase analysis, and optical microscopy.

Conflicts of Interest: The authors declare no conflict of interest.

References

1. Martinez-Marquez, D.; Delmar, Y.; Sun, S.; Stewart, R.A. Exploring macroporosity of additively manufactured titanium metamaterials for bone regeneration with quality by design: A systematic literature review. *Materials* **2020**, *13*, 4794. [CrossRef]
2. Grzeskowiak, R.M.; Schumacher, J.; Dhar, M.S.; Harper, D.P.; Mulon, P.Y.; Anderson, D.E. Bone and cartilage interfaces with orthopedic implants: A literature review. *Front. Surg.* **2020**, *7*, 601244. [CrossRef]
3. Oh, S.L.; Shiau, H.J.; Reynolds, M.A. Survival of dental implants at sites after implant failure: A systematic review. *J. Ecol. Eng.* **2020**, *123*, 54–60. [CrossRef] [PubMed]
4. Kenzhaliyev, B.K. Innovative technologies providing enhancement of non-ferrous, precious, rare and rare earth metals extraction. *Complex Use Miner. Resour.* **2019**, *310*, 64–75. [CrossRef]
5. Ramazanova, Z.; Zamalitdinova, M.; Kovalenko, M. Investigation of the properties of oxide coatings on titanium alloys obtained by plasma electrolytic oxidation. *Complex Use Miner. Resour.* **2022**, *321*, 5–13. [CrossRef]
6. Niespodziana, K.; Jurczyk, K.; Jakubowicz, J.; Jurczyk, M. Fabrication and properties of titanium–hydroxyapatite nanocomposites. *Mater. Chem. Phys.* **2010**, *123*, 160–165. [CrossRef]
7. Thian, E.S.; Loh, N.H.; Khor, K.A.; Tor, S.B. In vitro behavior of sintered powder injection molded Ti–6Al–4V/HA. *J. Biomed. Mater. Res.* **2002**, *63*, 79–87. [CrossRef]
8. Dorozhkin, S.V. Calcium orthophosphates. *J. Mater. Sci.* **2007**, *42*, 1061–1095. [CrossRef]
9. Ghiasi, B.; Sefidbakht, Y.; Mozaffari-Jovin, S.; Gharehcheloo, B.; Mehrarya, M.; Khodadadi, A.; Rezaei, M.; Siadat, S.O.R.; Uskokovi'c, V. Hydroxyapatite as a biomaterial—A gift that keeps on giving. *Drug Dev. Ind. Pharm.* **2020**, *46*, 1035–1062. [CrossRef]
10. Zakaria, S.M.; Zein, S.H.S.; Othman, M.R.; Yang, F.; Jansen, J.A. Nanophase Hydroxyapatite as a Biomaterial in Advanced Hard Tissue Engineering: A Review. *Tissue Eng. Part B Rev.* **2013**, *19*, 431–441. [CrossRef]

11. Mamayeva, A.; Kenzhegulov, A.; Kowalewski, P.; Wieleba, W. Investigation of hydroxyapatite-titanium composite properties during heat treatment. *Acta Bioeng. Biomech.* **2017**, *19*, 161–169.
12. Gross, K.A.; Berndt, C.C. Biomedical Application of Apatites. In *Phosphates: Geochemical, geobiological and Materials Importance Series: Reviews in Mineralogy and Geochemistry*; Kohn, M.J., Rakovan, J., Hughes, J.M., Eds.; Mineralogical Society of America: Washington, DC, USA, 2002; Volume 48, pp. 631–672.
13. Johnson, S.; Haluska, M.; Narayan, R.J.; Snyder, R.L. In situ annealing of hydroxyapatite thin films. *Mater. Sci. Eng.* **2006**, *26*, 1312–1316. [CrossRef]
14. Kathleen, M.H.G.; Connie, M.W. *Nutrition, Basic and Applied Bone Biology*, 2nd ed.; Academic Press: Cambridge, MA, USA, 2019; pp. 283–298.
15. Wang, L.; Wang, C.; Wu, S.; Fan, Y.; Li, X. Influence of the mechanical properties of biomaterials on degradability, cell behaviors and signaling pathways: Current progress and challenges. *Biomater. Sci.* **2020**, *8*, 2714–2733. [CrossRef]
16. Gurski, L.A.; Xu, X.; Labrada, L.N.; Nguyen, N.T.; Xiao, L.; van Golen, K.L.; Jia, X.; Farach-Carson, M.P. Hyaluronan (HA) interacting proteins RHAMM and hyaluronidase impact prostate cancer cell behavior and invadopodia formation in 3D HA-based hydrogels. *PLoS ONE* **2012**, *7*, e50075. [CrossRef]
17. Ma, G. Three common preparation methods of hydroxyapatite. *IOP Conf. Ser. Mater. Sci. Eng.* **2019**, *688*, 033057. [CrossRef]
18. Nakano, T.; Tokumura, A.; Umakoshi, Y. Variation in Crystallinity of Hydroxyapatite and the Related Calcium Phosphates by Mechanical Grinding and Subsequent Heat Treatment. *Metall. Mater. Trans. A* **2002**, *33A*, 521–528. [CrossRef]
19. Nakano, T.; Tokumura, A.; Umakoshi, Y.; Imazato, S.; Ehara, A.; Ebisu, S. Control of hydroxyapatite crystallinity by mechanical grinding method. *J. Mater. Sci. Mater. Med.* **2001**, *12*, 703–706. [CrossRef] [PubMed]
20. Dinda, S.; Bhagavatam, A.; Alrehaili, H.; Dinda, G.P. Mechanochemical synthesis of nanocrystalline hydroxyapatite from $Ca(H_2PO_4)_2$. H_2O, CaO, Ca $(OH)_2$, and P_2O_5 mixtures. *Nanomaterials* **2020**, *10*, 2232. [CrossRef] [PubMed]
21. Mamaeva, A.A.; Kenzhegulov, A.K.; Panichkin, A.V.; Shah, A. Obtaining hydroxyapatite coatings by mechanochemical interaction. *Complex Use Miner. Resour.* **2020**, *314*, 76–83. [CrossRef]
22. Arifin, A.; Sulong, A.B.; Muhamad, N.; Syarif, J.; Ramli, M.I. Material processing of hydroxyapatite and titanium alloy (HA/Ti) composite as implant materials using powder metallurgy: A review. *Mater. Des.* **2014**, *55*, 165–175. [CrossRef]
23. Ye, H.; Liu, X.; Hong, H. Characterization of sintered titanium/hydroxyapatite biocomposite using FTIR spectroscopy. *J. Mater. Sci. Mater. Med.* **2009**, *20*, 843–850. [CrossRef]
24. Chu, C.; Lin, P.; Dong, Y.; Xue, X.; Zhu, J.; Yin, Z. Fabrication and characterization of hydroxyapatite reinforced with 20 vol% Ti particles for use as hard tissue replacement. *J. Mater. Sci. Mater. Med.* **2002**, *13*, 985–992. [CrossRef]
25. Lu, Y.P.; Li, M.S.; Li, S.T.; Wang, Z.G.; Zhu, R.F. Plasma-sprayed hydroxyapatite + titania composite bond coat for hydroxyapatite coating on titanium substrate. *Biomaterials* **2004**, *25*, 4393–4403. [CrossRef]
26. Méndez-Rojas, M.A.; de la Rosa, L.A.G. Educational and Historical Aspects of Direct Synthesis of Metal Complexes. *Direct Synth. Met. Complexes* **2018**, 3–24. [CrossRef]
27. Ungar, T. Dislocation model of strain anisotropy. *JCPDS-Int. Cent. Diffr. Data* **2008**, *23*, 76–87. [CrossRef]
28. Nomura, N.; Sakamoto, K.; Takahashi, K.; Kato, S.; Abe, Y.; Doi, H.; Tsutsumi, Y.; Kobayashi, M.; Kobayashi, E.; Kim, W.-J.; et al. Fabrication and mechanical properties of porous Ti/HA composites for bone fixation devices. *Mater Trans.* **2010**, *51*, 1449–1454. [CrossRef]
29. Wang, Y.; Tang, S.; Ding, N.; Zhang, Z. Biological properties of hydroxyapatite coatings on titanium dioxide nanotube surfaces using negative pressure method. *J. Biomed. Mater. Res. Part B Appl. Biomater.* **2023**, *111*, 1365–1373. [CrossRef] [PubMed]
30. Nelea, V.; Morosanu, C.; Bercu, M.; Mihailescu, I.N. Interfacial titanium oxide between hydroxyapatite and TiAlFe substrate. *J. Mater. Sci. Mater. Med.* **2007**, *18*, 2347–2354. [CrossRef] [PubMed]
31. Rogina, A.; Košić, I.; Antunović, M.; Ivanković, M.; Ivanković, H. The bioactivity of titanium-cuttlefish bone-derived hydroxyapatite composites sintered at low temperature. *Powder Metall.* **2020**, *63*, 300–310. [CrossRef]

Disclaimer/Publisher's Note: The statements, opinions and data contained in all publications are solely those of the individual author(s) and contributor(s) and not of MDPI and/or the editor(s). MDPI and/or the editor(s) disclaim responsibility for any injury to people or property resulting from any ideas, methods, instructions or products referred to in the content.